Exome-wide Association Study Identifies *GREB1L* Mutations in Congenital Kidney Malformations

Simone Sanna-Cherchi,[1,27,*] Kamal Khan,[2] Rik Westland,[1,3] Priya Krithivasan,[1] Lorraine Fievet,[2] Hila Milo Rasouly,[1] Iuliana Ionita-Laza,[4] Valentina P. Capone,[1] David A. Fasel,[1] Krzysztof Kiryluk,[1] Sitharthan Kamalakaran,[5] Monica Bodria,[6] Edgar A. Otto,[7] Matthew G. Sampson,[8] Christopher E. Gillies,[8] Virginia Vega-Warner,[8] Katarina Vukojevic,[9] Igor Pediaditakis,[2] Gabriel S. Makar,[1] Adele Mitrotti,[1] Miguel Verbitsky,[1] Jeremiah Martino,[1] Qingxue Liu,[1] Young-Ji Na,[1] Vinicio Goj,[10] Gianluigi Ardissino,[11] Maddalena Gigante,[12] Loreto Gesualdo,[13] Magdalena Janezcko,[14] Marcin Zaniew,[15] Cathy Lee Mendelsohn,[16] Shirlee Shril,[17] Friedhelm Hildebrandt,[17] Joanna A.E. van Wijk,[3] Adela Arapovic,[18] Marijan Saraga,[18,19] Landino Allegri,[20] Claudia Izzi,[21,22] Francesco Scolari,[21] Velibor Tasic,[23] Gian Marco Ghiggeri,[6] Anna Latos-Bielenska,[24] Anna-Materna Kiryluk,[24] Shrikant Mane,[25] David B. Goldstein,[5] Richard P. Lifton,[25,26] Nicholas Katsanis,[2,27] Erica E. Davis,[2,27,*] and Ali G. Gharavi[1,27]

Renal agenesis and hypodysplasia (RHD) are major causes of pediatric chronic kidney disease and are highly genetically heterogeneous. We conducted whole-exome sequencing in 202 case subjects with RHD and identified diagnostic mutations in genes known to be associated with RHD in 7/202 case subjects. In an additional affected individual with RHD and a congenital heart defect, we found a homozygous loss-of-function (LOF) variant in *SLIT3*, recapitulating phenotypes reported with *Slit3* inactivation in the mouse. To identify genes associated with RHD, we performed an exome-wide association study with 195 unresolved case subjects and 6,905 control subjects. The top signal resided in *GREB1L*, a gene implicated previously in Hoxb1 and Shha signaling in zebrafish. The significance of the association, which was $p = 2.0 \times 10^{-5}$ for novel LOF, increased to $p = 4.1 \times 10^{-6}$ for LOF and deleterious missense variants combined, and augmented further after accounting for segregation and *de novo* inheritance of rare variants (joint $p = 2.3 \times 10^{-7}$). Finally, CRISPR/Cas9 disruption or knockdown of *greb1l* in zebrafish caused specific pronephric defects, which were rescued by wild-type human *GREB1L* mRNA, but not mRNA containing alleles identified in case subjects. Together, our study provides insight into the genetic landscape of kidney malformations in humans, presents multiple candidates, and identifies *SLIT3* and *GREB1L* as genes implicated in the pathogenesis of RHD.

Introduction

Congenital anomalies of the kidney and urinary tract (CAKUT [MIM: 143400]) are the predominant cause of end-stage renal disease (ESRD), requiring dialysis or transplantation in children and young adults.[1–7] Within the CAKUT phenotypic spectrum, renal agenesis and hypodysplasia (RHD [MIM: 191830]) are particularly severe conditions, affecting ~0.5% of the general population.[8–10] To date, more than 75 genes have been implicated in the causation of isolated or syndromic forms of RHD but collectively account for 10%–15% of cases. Both dominant and recessive inheritance of RHD have been described, and identified mutations include both point mutations and copy-number variations (CNVs).[11–21]

Because chronic kidney disease has a large impact on survival, extended families enabling traditional gene mapping are rare. In such a setting, the analysis of *de novo* mutations is a validated approach for gene discovery but requires ascertainment of parent-child trios. However, in

[1]Division of Nephrology, Columbia University, New York, NY 10032, USA; [2]Center for Human Disease Modeling, Duke University, Durham, NC 27701, USA; [3]Department of Pediatric Nephrology, VU University Medical Center, Amsterdam 1007 MB, the Netherlands; [4]Department of Biostatistics, Columbia University, New York, NY 10032, USA; [5]Institute for Genomic Medicine, Columbia University Medical Center, New York, NY 10032, USA; [6]Division of Nephrology, Dialysis, Transplantation, and Laboratory on Pathophysiology of Uremia, Istituto G. Gaslini, Genoa 16147, Italy; [7]University of Michigan School of Medicine, Department of Internal Medicine-Nephrology, Ann Arbor, MI 48109, USA; [8]University of Michigan School of Medicine, Department of Pediatrics-Nephrology, Ann Arbor, MI 48109, USA; [9]Department of Anatomy, Histology, and Embryology, School of Medicine, University of Split, Split 21000, Croatia; [10]Pediatric Unit, Fatebenefratelli Hospital, Milan 20121, Italy; [11]Pediatric Nephrology and Dialysis Unit, Fondazione Ca' Granda IRCCS Ospedale Maggiore Policlinico Milano, 20122 Milan, Italy; [12]Department of Medical and Surgical Sciences, University of Foggia, Foggia 71121, Italy; [13]Section of Nephrology, Department of Emergency and Organ Transplantation, University of Bari, Bari 70121, Italy; [14]Department of Medical Genetics, Chair of Pediatrics, Jagiellonian University, Collegium Medicum, Krakow 31-008, Poland; [15]Children's Hospital, Poznan 61-825, Poland; [16]Department of Urology, Pathology and Cell Biology, Genetics and Development, Columbia University, New York, NY 10032, USA; [17]Department of Medicine, Boston Children's Hospital, Harvard Medical School, Boston, MA 02115, USA; [18]Department of Pediatrics, University Hospital of Split, Split 21000, Croatia; [19]School of Medicine, University of Split, Split 21000, Croatia; [20]Department of Medicine and Surgery, University of Parma, Parma 43100, Italy; [21]Cattedra di Nefrologia, Università di Brescia, Seconda Divisione di Nefrologia Azienda Ospedaliera Spedali Civili di Brescia Presidio di Montichiari, Brescia 25018, Italy; [22]Dipartimento Ostetrico Ginecologico, Azienda Ospedaliera Spedali Civili di Brescia, Brescia 25018, Italy; [23]Department of Pediatric Nephrology, University Children's Hospital, Medical Faculty of Skopje, Skopje 1000, Macedonia; [24]Department of Medical Genetics, Poznan University of Medical Sciences, and Center for Medical Genetics GENESIS, Poznan 61-701, Poland; [25]Department of Human Genetics, Yale University School of Medicine, New Haven, CT 06510, USA; [26]Howard Hughes Medical Institute, Chevy Chase, MD 20815, USA
[27]These authors contributed equally to this work
*Correspondence: ss2517@cumc.columbia.edu (S.S.-C.), erica.davis@duke.edu (E.E.D.)
https://doi.org/10.1016/j.ajhg.2017.09.018.

the absence of parental biospecimens, exome-wide case-control association studies using gene-level collapsing approaches are emerging as a cost-efficient and powerful alternative for identifying rare variants with large effect on disease.[22–29] These studies are founded on the population genetic prediction that disease-causing variants for traits that impact survival will be under strong purifying selection and will be extremely rare or absent in the general population. With the availability of large population databases such as Exome Aggregation Consortium (ExAC),[30] population-specific polymorphisms can be filtered rapidly from case and control subjects, thereby restricting the association analysis to exceedingly rare variants that are most likely to impart a large risk on disease phenotype. Once a gene has been identified by collapsing analysis, one can evaluate each qualifying variant that drives this signal and conduct additional tests, such as segregation in available family members and functional modeling in cellular or animal systems to test function.

Here, we report dominant LOF mutations in *GREB1L* as a cause for severe renal malformations, demonstrating that even with modest case sample size, exome-wide collapsing analysis for ultra-rare variants can lead to the identification of Mendelian dominant alleles for developmental traits characterized by high genetic heterogeneity.

Subjects and Methods

Study Samples

We studied 612 individuals affected by RHD (Table S1) and 6,905 control subjects. For 202 RHD-affected case subjects, we performed whole-exome sequencing (WES); for an additional 410 case subjects, we performed targeted next-generation sequencing for *GREB1L*. All 202 RHD-affected case subjects were subjected initially to DNA microarrays for exclusion of pathogenic CNVs as described.[14–17] All control subjects were subjected to WES. Written informed consent was obtained from all the participants. The study was approved by the Institutional Review Board at each site.

As controls, we used 6,905 exomes performed on individuals undergoing WES at the Columbia Institute of Genomic Medicine (IGM) for indications unrelated to kidney disease. These included healthy parents of children referred for various neurological and metabolic disorders (Table S2).

Whole-Exome Sequencing

WES was performed on 202 RHD-affected case subjects through the Yale Center for Mendelian Genomics as described.[11,14,31,32] In brief, for each capture experiment, 3 μg of genomic DNA was fragmented, linkers were ligated to the ends, and a library was prepared. Genomic DNA was annealed to Roche V2 capture probes, and bound genomic DNA was eluted and subjected to sequencing. Next-gen sequencing was then performed on an Illumina HiSeq 2500 machine. Sequence reads were converted to FASTQ format and mapped to the reference genome. We used uniform procedures for variant calling in case and control subjects to avoid introduction of technical bias in the study. Exome samples in both case and control subjects were processed using a consistent alignment and variant calling pipeline, consisting of primary alignment using bwa-0.5.10, duplicate removal using Picard tools, index realignment and variant calling using GATK 3.6, and variant annotation using snpEff-3.3, AnnoVar, and SeattleSeq, with Ensembl-GRCh37.73 annotations.

Targeted Next-Generation Sequencing

High-throughput next-generation sequencing for *GREB1L* was conducted in 410 additional RHD-affected case subjects using the Fluidigm microfluidic PCR capture coupled to next-generation sequencing on a HiSeq 2500 (Illumina) as described.[33,34] In brief, to cover all 33 coding exons and intron/exon boundaries of *GREB1L*, we designed target-specific primer pairs according to the guidelines of the Access Array user guide (Fluidigm). The maximal amplicon size is set to 290 bp anticipating subsequent NGS paired-end reads of 2 × 150 bases. Universal primer sequences required for Illumina-compatible amplicon tagging and for downstream indexing were added at the 5′ end of all target-specific primers. We then generated 48 × 10-plex primer pools. 48 DNA-containing samples were combined with each of the 48 primer solutions into 2,304 separate microreaction chambers. PCR products were then harvested and transferred to a 96-well microtiter-plate. In a second PCR reaction, Illumina sequence-specific adaptors and sample barcodes were attached. We indexed up to 96 total DNA samples by attaching 96 different barcodes after processing 2 different 48.48 Access Arrays. Subsequently, all 96 barcoded samples were pooled and submitted for next-generation sequencing on a single lane of an Illumina HiSeq 2500 instrument. To sequence the Fluidigm-specific barcodes and perform a multiplexed paired-end run, we substituted the Illumina index sequencing primer with custom Fluidigm-specific index primer and extended the index read length to decipher the whole Fluidigm barcode. Analysis of targeted resequencing and variant calling was performed using TarSVM, a support vector machine-based algorithm specifically designed to assess microfluidic PCR-derived next-generation sequencing data.[35]

Clinical Annotation and Variant Prioritization

After exome or targeted resequencing, all variants were annotated based on their predicted effect on protein function using Annovar[36] and SnpEff[37] annotation software. Allelic frequencies were estimated based on public databases including ExAC, gnomAD, dbSNP, and the 1000 Genomes Project, as well as 6,905 internal control subjects. Prediction of pathogenicity was computed using algorithms such as PolyPhen[38] and Combined Annotation Dependent Depletion (CADD).[39] Additional resources for facilitating variant interpretation and establishing genetic causality included ClinVar, the Human Gene Mutation Database (HGMD), Online Mendelian Inheritance in Man (OMIM), and an in-house curated list of genes known to be associated to human or mouse models of CAKUT, followed by systematic review of the literature. Clinical interpretation of variants was based on American College of Medical Genetics (ACMG) recommendations.[40] All listed variants in Tables 1, 3, and S3 were confirmed by Sanger sequencing according to standard protocols.

Case-Control WES Harmonization and Collapsing Analysis for Rare Variants Association

We conducted extensive QC and harmonization analyses between case and control exomes to minimize spurious results as well as

Table 1. Diagnostic Variants in Established CAKUT Genes Identified in the Discovery Cohort

Chr:position (hg19)	Gene	Variant	Consequence	CADD	CUMC controls MAF (%)	ExAC MAF (%)	Reported as Pathogenic	OMIM Syndrome	Case	Sex	CAKUT Phenotype	Side (L, R, B)	Additional CAKUT Phenotype	Extrarenal Phenotype	Family History	Inheritance
8:72127888	*EYA1*	c.1436T>A	p.Leu479*	45.0	0	0	NA	branchio-otic syndrome 1 (602588)	DC1	M	renal hypoplasia	B	–	BOR syndrome features	Y (info NA)	father
10:8106047	*GATA3*	c.872_873delAT	p.Tyr291Serfs*12	NA	0	0	NA	hypoparathyroidism sensorineural deafness and renal dysplasia (146255)	DC2	F	renal hypoplasia	L	–	synechiae vulvae	Y (paternal side with chronic kidney disease)	NA
10:102509646	*PAX2*	c.187G>A	p.Gly63Ser	34.0	0	0	ClinVar Pathogenic	papillorenal syndrome (120330)	DC3	M	renal agenesis	L	–	–	Y (mother with RHD)	*de novo*
10:102568963	*PAX2*	c.892_895delGGCA	p.Gly298Hisfs*7	NA	0	0	NA	papillorenal syndrome (120330)	DC4	F	renal hypoplasia	B	cysts	bilateral nervus opticus coloboma, atrial septum defect, obesity	NA	father
16:20359916	*UMOD*	c.707C>G	p.Pro236Arg	25.9	0	0	HGMD[a]	medullary cystic kidney disease 2 (603860)	DC5	M	renal hypoplasia	B	VUR, hydronephrosis	hyperuricaemia	Y (mother and brother with RHD)	NA
17:36099434	*HNF1B*	c.541C>T	p.Arg181*	37.0	0	0	Clinvar pathogenic/ HGMD[a]	renal cysts and diabetes syndrome (137920)	DC6	M	multicystic dysplastic kidney	B	VUR	epispadia	N	*De novo*
19:46271428	*SIX5*	c.675C>A	p.Tyr225*	37.0	0	0	NA	branchio-oto-renal syndrome (610896)	DC7	M	renal dysplasia	L	–	–	N	Mother

Abbreviations are as follows: B, bilateral; BOR, branchio-oto-renal; CADD, combined annotation dependent depletion score; CAKUT, congenital anomalies of the kidney and urinary tract; CUMC, Columbia University Medical Center; del, deletion; ExAC, Exome Aggregation; F, female; fs, frameshift; M, male; HGMD, human gene mutation database; L, left; MAF, minor allele frequency; NA, not available; OMIM, online Mendelian inheritance in man; R, right; RHD, renal hypodysplasia; VUR, vesicoureteral reflux.
[a]HGMD references.[66,67]

Table 2. Top Signals Identified from the Loss-of-Function Variant Burden Test between 195 RHD-Affected Case Subjects and 6,905 Control Subjects

Rank	Gene	Total Qualifying Variants in 195 Case Subjects	Total Qualifying Variants in 6,905 Control Subjects	Frequency of Qualifying Variants in Case Subjects	Frequency of Qualifying Variants in Control Subjects	Frequency of Loss-of-Function Alleles in ExAC Database	OR (95% CI) (Cases versus Controls)	p Value (Cases versus Controls)
1	*GREB1L*	3	0	0.0154	0	4.41×10^{-5}	Inf (14.7-inf)	2.04×10^{-5}
2	*VPS28*	2	0	0.0103	0	2.60×10^{-4}	Inf (6.7-inf)	7.51×10^{-4}
3	*MFN1*	2	0	0.0103	0	2.25×10^{-4}	Inf (6.7-inf)	7.51×10^{-4}
4	*BCORL1*	2	0	0.0103	0	1.19×10^{-4}	Inf (6.7-inf)	7.51×10^{-4}
5	*ZBTB3*	2	1	0.0103	1.45×10^{-4}	1.08×10^{-4}	71.3 (3.7-4077)	0.0022
6	*SLC39A6*	2	1	0.0103	1.45×10^{-4}	1.25×10^{-4}	71.3 (3.7-4077)	0.0022
7	*SUCLG1*	2	1	0.0103	1.45×10^{-4}	1.55×10^{-3}	71.3 (3.7-4077)	0.0022
8	*MYOT*	2	1	0.0103	1.45×10^{-4}	2.73×10^{-4}	71.3 (3.7-4077)	0.0022
9	*ZNF277*	2	1	0.0103	1.45×10^{-4}	3.48×10^{-3}	71.3 (3.7-4077)	0.0022
10	*CCDC81*	2	2	0.0103	2.90×10^{-4}	1.41×10^{-3}	35.7 (2.6-488.8)	0.0043
11	*GCC2*	2	2	0.0103	2.90×10^{-4}	7.85×10^{-4}	35.7 (2.6-488.8)	0.0043

Presented are the 11 highest ranked genes ($p < 5 \times 10^{-3}$) that have qualifying heterozygous loss-of-function variants enriched in case subjects versus control subjects on the basis of whole-exome sequencing collapsing analysis. p value is calculated using Fisher's exact test. Abbreviations are as follows: CI, confidence interval; ExAC, Exome Aggregate Consortium database; inf, infinite; OR, odds ratio.

false negative findings due systematic bias from multiple sources including capture platform and sequencing, as well as population structure. This method was successfully used for similarly designed case-control WES studies on amyotrophic lateral sclerosis and idiopathic pulmonary fibrosis to identify disease-causing genes.[22,23] After variant calling using uniform procedures, resulting calls and their underlying quality statistics were then stored in a database of variants (AnnoDB) that powers the Analysis Tool for Annotated Variants (ATAV) analyses. ATAV is designed to detect complex disease-associated rare genetic variants by performing association analysis on annotated variants derived from whole-genome sequencing or WES data stored in AnnoDB (see Web Resources). After we ensured that the alignment and variant call data were obtained exactly the same way, we next verified that all variant calls in samples involved in an analysis were of comparable quality and each consensus coding sequence (CCDS) exon has adequate coverage between case and control subjects. Coverage data were parsed from a compressed mpileup file generated by the main alignment/genotyping pipeline, transformed into an optimized binned text-based format, and bulk-loaded to servers. Coverage values were coded as one of five possible values (<3×, 3–9×, 10–19×, 20–200×, or >201×) calculated in windows of 10,240 bp. We next performed site-level coverage harmonization across genes to enable our collapsing analysis framework to control for potential with differential sequence coverage between case and control subjects. First, the number of bases with at least 10× coverage was calculated for each CCDS exon plus 10 bp into each intron for each sample. Next, we selected bases with similar mapping qualities and a minimum depth of coverage of 10× in case and control subjects, and we removed sites that were differentially captured and sequenced in both case and control subjects. Using this harmonization procedure, each CCDS site that showed an absolute difference in the percentage of case subjects covered at 10× compared to control subjects of greater than 6% was excluded. The pruning of differentially covered sites resulted in retention of 30.42 Mb of CCDS sequence (91.5%) for case-control collapsing analysis. We then selected qualifying variants based on the following criteria: (1) quality thresholds including read depth >10×, mapping quality >40, genotype quality >50, quality by depth >2; (2) predicted functional consequence, selecting CCDS variants predicted to result in amino acid change or a LOF (defined as frameshift, stop-gain, or splice site variant); (3) absence in external population databases in ExAC, gnomAD, NHLBI Exome Sequencing Project (ESP) Exome Variant Server (EVS); and (4) low frequency in our combined case and control dataset (minor allele frequency [MAF] < 0.000141; i.e., we did not allow for any variant to be observed more than once in either the case subjects, the control subjects, or the case and control subjects together). The primary analyses involved burden tests using two models: (1) LOF variants in case and control subjects (Table 2) and (2) case-control burden for LOF plus deleterious nonsynonymous missense variants (extended model to incorporate ultra-rare missense variants with MAF = 0 predicted to be deleterious based on CADD score > 20; Table S5). To test robustness of our results, we conducted another burden analysis involving genetic matching of case and control subjects; we selected 8,749 individual autosomal markers with a MAF > 1% that were not in linkage disequilibrium ($R^2 < 0.2$) to perform principal component analysis using smartpca.[41] We removed 2,787 control subjects after genetic matching to establish a final dataset of 195 case subjects and 4,118 control subjects (Table S6). All these analyses were conducted under a dominant model.

To incorporate inheritance information into our collapsing/burden test statistics for *GREB1L*, we computed the joint probability and p value for association (Fisher's exact test) with the transmission for segregating and *de novo* mutations using the formula "-2*ln(Fisher's P-val)-2*ln(LOD score P-val)-2*ln(*de novo* P-val) ~chisquare(6 df)." The LOD score p value for four informative meioses under an autosomal-dominant model with rare disease allele frequency is 0.00936. The expected probability "mu" of *de novo* missense mutations in *GREB1L* was estimated based on

Samocha et al.[42] Since *GREB1L* does not have an absolute estimate of *de novo* mutations, we computed the probability of *de novo* missense by using 307 genes with CCDS size comparable to *GREB1L* (for which probabilities were available) and obtained a point estimate of 6.6×10^{-5} (1 SD range 5.2×10^{-5} to 8.4×10^{-5}). As a conservative measure, we assumed as if we had trio data available for all 195 index case subjects, then the probability of observing at least one *de novo* in 195 independent trios was P(X > = 1) where X~Poisson(2*195*mu) = 0.0254.

Transient Suppression of *greb1l* and *In Vivo* Complementation Studies in Zebrafish

All studies performed in zebrafish were approved by the Duke University Institutional Animal Care and Use Committee (IACUC). Reciprocal blast of human GREB1L (GenBank: NP_001136438.1) against the *D. rerio* genome identified a single zebrafish ortholog (61% amino acid identity; 73% similarity). We designed a splice blocking morpholino (MO) targeting the splice donor site of exon 17 (5′-CACATAGCTGCATCTCTCACCTTGT-3′; Gene Tools; Figure S3A). To determine MO efficiency, we injected 4 ng MO in WT (Ekkwill, EK) zebrafish embryos (1 nL/embryo) obtained by natural mating at the 1- to 4-cell stage and harvested embryos at 2 days post-fertilization (dpf) for RNA extraction. We extracted total RNA with Trizol (Invitrogen) according to manufacturer's instructions. We performed RT-PCR with resulting RNA using the QuantiTect Reverse Transcription kit (QIAGEN), amplified the region flanking the MO target site, and migrated it on a 1% agarose gel (Figure S3B). PCR fragments were extracted from the gel (QIAquick gel extraction kit, QIAGEN) and cloned using the TOPO TA cloning kit for sequencing (ThermoFisher). Individual colonies were Sanger sequenced according to standard protocols and analyzed with Lasergene software (DNASTAR) to characterize aberrant splicing. We optimized *in vivo* complementation assays with a MO dose curve (1 ng, 2 ng, 3 ng, 4 ng; 45–50 embryos/batch; repeated; Figure S3D), and all subsequent assays were conducted with 2 ng MO. To rescue MO phenotypes, we obtained a custom-synthesized WT human *GREB1L* open reading frame (ORF) construct corresponding to GenBank: NM_001142966.2 (GeneArt, ThermoFisher) and cloned it into the pCS2+ vector backbone using LR clonase II recombination (ThermoFisher). We conducted site-directed mutagenesis as described[43] and generated capped mRNA with the mMessage mMachine SP6 kit (ThermoFisher) using linearized plasmid as a template. To rescue MO phenotypes or test the effect of mRNA alone, we injected 200 pg *GREB1L* WT or mutant mRNA for all experiments.

CRISPR/Cas9 Genome Editing of *greb1l* in Zebrafish

We used ChopChop to design two non-overlapping single guide RNAs (sgRNA) targeting exons 8 and 10 of *greb1l* (GRCz10 Ensembl Transcript ID: ENSDART00000057268.6; exon 8, 5′-GGATGAGCCAGATTGCATGC-3′ and exon 10, 5′-CGACAGGTCCACCAAAAAAG-3′; Figure S3A). We synthesized sgRNAs using the Gene Art precision gRNA synthesis Kit (Invitrogen) per manufacturer's instructions. To test sgRNA efficiency, we co-injected 100 pg sgRNA with 200 pg Cas9 protein (PNA Bio) into zebrafish embryos (WT; Ekkwill, EK) at the 1-cell stage and we assessed (1) percentage of embryos targeted and (2) estimated mosaicism in individual embryos as described.[44] Briefly, we harvested F0 mutant embryos at 2 dpf for genomic DNA extraction using proteinase K (Life technologies) digestion, and we PCR amplified regions flanking the sgRNA targets. To assess percentage of embryos targeted, we performed heteroduplex analysis of the amplified product by heat denaturation and slow reannealing (95°C for 5 min, ramp down to 85°C at −1°C/s, and then to −0.1°C/s). We migrated resulting products corresponding to F0 mutants (n = 8–10) and uninjected controls (n = 2) on a precast 15% polyacrylamide gel (ThermoFisher) and visualized it post-migration with ethidium bromide staining and a UV lamp. To estimate mosaicism, we cloned PCR products using the TOPO TA cloning kit for sequencing (ThermoFisher) and Sanger sequenced 16–24 colonies per embryo corresponding to 4 mutants and 1 control embryo per sgRNA. We cataloged indels proximal to the protospacer adjacent motif (PAM) using DNAStar (Lasergene).

Assessment of the Zebrafish Proximal Convoluted Tubule

To assess the proximal renal convoluted tubule in morphants and mutants, we conducted whole-mount immunostaining with an antibody against Na^+-K^+-ATPase alpha-1 subunit (a6F, DSHB) as described.[14,45] Briefly, the larval batches were fixed at 4 dpf in Dent's solution (80% methanol, 20% dimethylsulfoxide) overnight at 4°C. We rehydrated larvae with a decreasing series of methanol and phosphate-buffered saline with 0.1% TWEEN-20 (PBST); rehydrated larvae were then washed with PBST (0.1% Tween). The pronephros was then stained with primary antibody (a6F, Developmental Studies Hybridoma B 1:20 dilution) and goat anti-mouse IgG secondary antibody (488 Alexa Fluor, Invitrogen; 1:500 dilution). We acquired lateral images with an AZ100 florescent microscope (Nikon), digital sight black and white camera (Nikon), and NIS Elements software (Nikon) at 4× magnification. We measured the area of the proximal renal convoluted tubule with ImageJ (NIH) and determined statistical differences between pairs of batches with an unpaired t test (GraphPad software; see Table S7). Measurements were normalized to control embryos.

Results

Exome Sequencing Identifies Diagnostic Mutations in the Minority of RHD-Affected Case Subjects from Our Cohort

To identify disease-causing mutations in genes previously associated with Mendelian forms of CAKUT, we annotated all high-quality variants in our 202 RHD-affected case subjects and 6,905 internal exome control subjects (Tables S1 and S2) based on the following criteria: (1) located within genes previously associated to CAKUT or CAKUT phenocopies in humans; (2) absent or exceedingly rare (MAF < 0.001) in population controls (ExAC, gnomAD, 1000 Genomes project); (3) protein-changing alterations (stop gain, splice, frameshift, nonsynonymous changes) predicted to be deleterious according to the CADD score; (4) reported to be pathogenic for human kidney phenotype in clinical databases (ClinVar pathogenic or likely pathogenic; HGMD pathogenic); and (5) occurring *de novo* in simplex case subjects or segregating in any available affected relatives.

We identified pathogenic mutations in 7/202 RHD-affected individuals based on ACMG criteria (3.5% of the study cohort). These mutations mapped to five genes known to be implicated in CAKUT (*EYA1* [MIM: 601653],

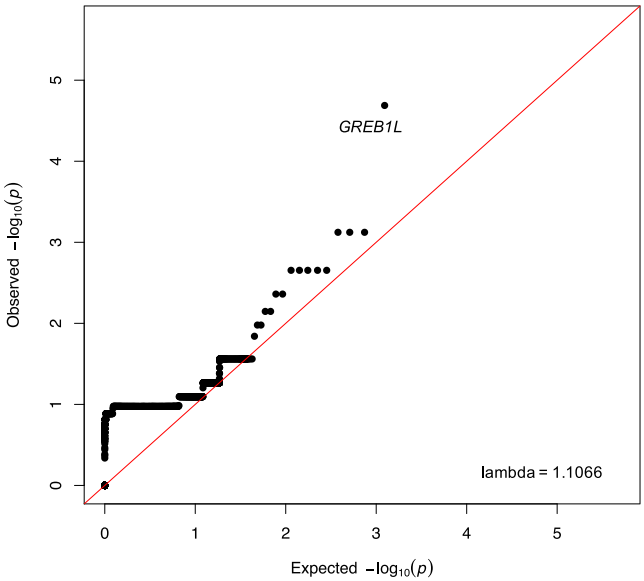

Figure 1. Quantile-Quantile (QQ) Plot
Expected versus observed p values of the rare loss-of-function model for whole-exome sequencing collapsing analysis in 195 RHD-affected case subjects and 6,905 control subjects. The signal for *GREB1L* is indicated.

GATA3 [MIM: 131320], *PAX2* [MIM: 167409], *HNF1B* [MIM: 189907], and *SIX5* [MIM: 600963]),[46–50] as well as a mutation in *UMOD* (MIM: 191845), which can produce a phenocopy of CAKUT (Table 1). Guided by these mutations, clinical follow-up corrected the classification of two case subjects predicted to have a syndromic disease (Branchio-oto-renal [BOR] syndrome [MIM: 113650] in case DC1; renal coloboma syndrome [MIM: 120330] in case DC4) and also uncovered rare phenotypic associations (atrial septum defect, macrosomia, and obesity in case DC4; epispadias in case DC6). Other identified rare variants in CAKUT genes that did not meet the ACMG criteria for pathogenicity were classified as variants of unknown significance (VUS).

Identification of Rare Variants that Define Possible Phenotypic Expansion of Known Syndromes, Phenocopies of RHD, or Affecting Genes whose Inactivation Results in CAKUT in the Mouse

Next, we annotated our exome data for mutations in genes implicated in human malformation syndromes that sometimes include genitourinary defects as part of their clinical spectrum, as well as genes whose inactivation results in CAKUT in the mouse. We identified 28 rare variants in 18 genes (absent or exceedingly rare in public databases such as ExAC and gnomAD, as well as in our internal 6,905 control subjects) in 26 independent RHD-affected case subjects (Tables S3 and S4). In particular, we identified a homozygous frameshift variant (c.1193delC, resulting in the protein change p.Thr398Serfs*37) in *SLIT3* (MIM: 603745), in a European case subject with complex CAKUT and patent foramen ovale. The variant is absent in all databases and our control subjects, and the alleles were transmitted by two heterozygous, unaffected parents. The targeted inactivation of *Slit3* in the mouse causes congenital diaphragmatic hernia, cardiac defects, and renal agenesis or hypoplasia.[51] These findings thus nominate biallelic mutations in *SLIT3* as a recessive cause of syndromic CAKUT in humans.

We also highlight four individuals harboring LOF variants in *WNT5A* (MIM: 164975), *SETBP1* (MIM: 611060), *T* (MIM: 601397), and *HSPA4L* because mutations in these genes have been reported to cause multi-organ defects, including the urinary tract, in humans or mice.[52–55] However, the patients harboring these LOF variants had only isolated kidney malformations and therefore, owing of the lack of statistical evidence, incomplete match with expected phenotypes, and absence of functional studies, these genes were classified as candidates, requiring further investigation of causality in larger cohorts.

Rare Variant Collapsing Analysis and Segregation Studies Identify *GREB1L* as a Susceptibility Gene for RHD

To identify susceptibility genes for RHD, we performed an exome-wide case-control association study in the 195 RHD-affected case subjects without a definitive genetic diagnosis and our 6,905 control subjects. Our study focused on gene-based collapsing analysis of rare variants, a robust method for discovery of mutations contributing to disease.[22–24] To achieve this, we first conducted extensive quality control (QC) and we performed site harmonization to avoid spurious findings due to imbalance in sequence coverage between case and control subjects (see Subjects and Methods). After elimination of differentially covered sites, we excluded 8.5% of the bases, providing a total of 30.42 Mb of CCDS exons for collapsing analyses. After pruning, case and control subjects had 96.051% and 96.3% of CCDS bases covered at 10× or more, respectively. Because RHD is rare and heterogeneous, we modeled dominant inheritance of ultra-rare, highly deleterious variants, with qualifying variants defined as LOF and predicted deleterious nonsynonymous variants that are absent in ExAC, dbSNP, and the 1000 Genomes Project. The analysis of rare LOF variants yielded 11 genes with a Fisher's exact test p value $< 5.0 \times 10^{-3}$ and minimal genomic inflation (Table 2, Figure 1). The top signal was *GREB1L*, which harbored three heterozygous LOF variants in 195 case subjects (two stop-gain and one frameshift, 1.5% of case subjects) and zero LOF variants in 6,905 control subjects ($p = 2.0 \times 10^{-5}$; OR = inf). Among the top 11 signals, *GREB1L* was the gene most depleted by LOF mutations in ExAC and gnomAD. *GREB1L* is also ranked in the top 0.04^{th} percentile among the most negatively selected genes, as measured by the Gene-level integrated Metric of Negative Selection.[56] The analysis of aggregate rare LOF and deleterious nonsynonymous variants yielded a near exome-wide significant signal for *GREB1L* ($p = 4.1 \times 10^{-6}$; OR 8.7, 95% CI 3.66–18.72; Table S5). The *GREB1L* signal was not influenced by population structure, since the results

Table 3. Rare Heterozygous *GREB1L* Variants Identified in the Discovery and Additional Cohorts

Chr:position (hg19)	Variant	Consequence	CADD	CUMC Controls MAF (%)	ExAC MAF (%)	Case	Sex	CAKUT Phenotype	Side (L, R, B)	Additional CAKUT Phenotype	Extrarenal Phenotype	Family History	Inheritance
18:18963516	c.37C>T	p.Arg13*	37.0	0	0	DC8	M	multicystic dysplastic kidney	L	congenital megaureter	–	Y (maternal side, phenotype NA)	NA
18:18975373	c.383G>A	p.Arg128His	34.0	0	0	DC9	F	renal agenesis	L	–	unicornate uterus, agenesis of left ovary	Y (info NA)	NA
18:19053090	c.2281G>C	p.Glu761Gln	23.8	0	0	DC10	F	renal dysplasia	L	duplication of the ureter	–	Y (uncle with double collecting system)	father
18:19076465	c.3197G>C	p.Arg1066Pro	34.0	0	0	DC11	F	renal agenesis	L	–	–	N	NA
18:19080529	c.3998_3999insC	p.Leu1334Profs*18	NA	0	0	DC12	F	renal agenesis	R	–	–	Y (mother with RHD)	affected mother
18:19088497	c.4680C>A	p.Tyr1560*	45.0	0	0	DC13	M	renal agenesis	B	bladder agenesis	Potter sequence	Y	affected sister (VUR), mother (uterus anomaly)
18:19088517	c.4700T>C	p.Leu1567Pro	28.2	0	0	DC14	F	renal agenesis	L	–	–	N	*de novo*
18:19095467	c.4991A>C	p.Tyr1664Cys	28.0	0	0	DC15	M	renal agenesis	L	–	–	N	NA
18:19095544	c.5068G>A	p.Val1690Met	29.6	0	0	DC16	F	renal agenesis	L	–	–	Y (sister with VUR)	affected sister (VUR), father (affection status unknown)
Additional Cohort													
18:18983941	c.818G>T	p.Gly273Val	13.9	0	0	AC1	M	renal agenesis	L	–	–	N	NA
18:19029567	c.1490C>G	p.Ala497Gly	14.5	0	0	AC2	F	renal agenesis	R	–	–	N	NA
18:19053090	c.2281G>C	p.Glu761Gln	26.8	0	0	AC3	M	multicystic dysplastic kidney	R	congenital megaureter	–	N	father
18:19076563	c.3295C>T	p.Gln1099*	40.0	0	0	AC4	F	multicystic dysplastic kidney	R	–	–	Y (mother with RHD)	affected mother
18:19088463	c.4646T>C	p.Val1549Ala	27.9	0	0	AC5	F	renal agenesis	L	–	agenesis of the uterus, Henoch Schönlein Purpura	N	NA
18:19093889	c.4843G>A	p.Val1615Ile	22.2	0	0	AC6	F	renal dysplasia	B	congenital hydronephrosis		Y (two first cousins have VUR, side of family NA)	mother
18:19095440	c.4964T>C	p.Ile1655Thr	22.6	0	0	AC7	F	renal agenesis	L	–	genua valga, flat feet, right neurosensorial hypoacusia	N	father
18:19102661	c.5651G>A	p.Arg1884His	28.6	0	0	AC8	M	renal hypoplasia	L	–	–	N	NA

Abbreviations are as follows: B, bilateral; CADD, combined annotation dependent depletion score; CAKUT, congenital anomalies of the kidney and urinary tract; CUMC, Columbia University Medical Center; del, deletion; ExAC, Exome Aggregation Consortium; F, female; fs, frameshift; L, left; M, male; MAF, minor allele frequency; NA, not available; RHD, renal hypodysplasia; R, right; VUR, vesicoureteral reflux. GREB1L RefSeq ID: NM_001142966.2.

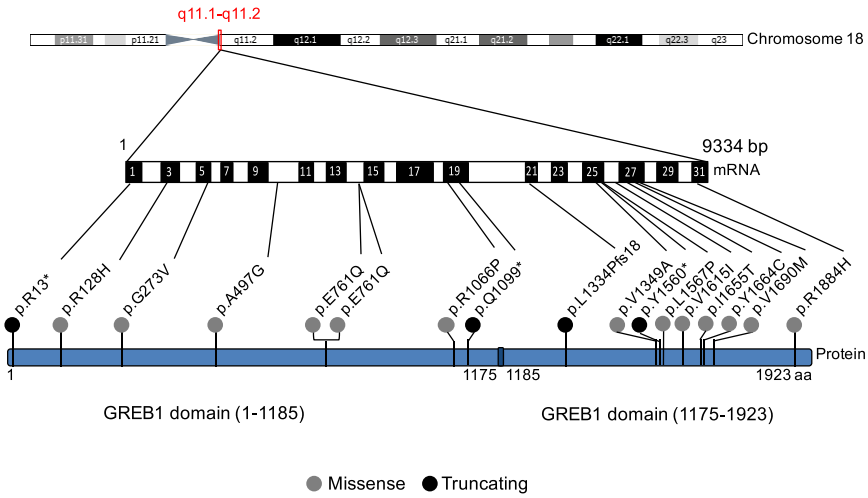

Figure 2. Spatial Overview of the Qualifying *GREB1L* Heterozygous Variants Discovered in Our RHD Cohort

The lollipops in black and gray indicate loss-of-function mutations and non-synonymous mutations, respectively. Numbers on the mRNA schematic indicate the coding exons in *GREB1L*; numbers on the protein schematic indicate amino acid numbers. The abbreviated variant names correspond to the following amino acidic substitutions: p.Arg13*, p.Arg128His, p.Glu761Gln, p.Arg1066Pro, p.Leu1334Profs*18, p.Tyr1560*, p.Leu1567Pro, p.Tyr1664Cys, p.Val1690Met, p.Gly273Val, p.Ala497Gly, p.Glu761Gln, p.Gln1099*, p.Val1549Ala, p.Val1615Ile, p.Ile1655Thr, p.Arg1884His.

were robust to secondary analyses using case and control subjects matched by principal component analysis (PCA) ($p = 3.0 \times 10^{-6}$, OR 9.9, 95% CI 3.9–23.1; Table S6).

Altogether, we identified previously unreported deleterious *GREB1L* variants (three LOF, six missense) in 9/195 (4.6%) of case subjects (Table 3 and Figure S1). Parent and family member DNAs were available for four individuals harboring mutations. In three of them (two LOF and one missense), the mutation segregated in affected individuals following a dominant model. Moreover, the c.4700T>C (p.Leu1567Pro) substitution, present in a case subject with isolated unilateral renal agenesis and unaffected parents, occurred *de novo* (Figure S1E). These data strongly implicate dominant mutations in *GREB1L* as a cause of RHD. *A posteriori* calculation of the joint probabilities based on exome-wide collapsing analysis with segregation and *de novo* occurrence yielded a highly significant combined p value of 2.3×10^{-7}.

Additional Deleterious *GREB1L* Mutations Detected in an Independent Cohort

To test the genetic contribution of *GREB1L* in RHD further, we conducted a targeted resequencing study using microfluidic PCR enrichment and coupled to next-generation sequencing (Fluidigm) to screen the 33 exons (31 coding, 2 noncoding) of *GREB1L* in an additional 410 independent RHD-affected case subjects as previously described.[14,33,34] We identified additional novel heterozygous mutations (one LOF and seven predicted deleterious missense variants) in eight case subjects (2.0%, Table 3). The LOF variant c.3295C>T (p.Gln1099*) was detected in a case subject with unilateral multicystic dysplastic kidney and was inherited from an affected mother with renal hypodysplasia (Figure S1B). Thus, in aggregate, we identified previously unreported deleterious mutations (4 LOF and 13 missense, Figure 2) in 17/605 RHD-affected case subjects from our two cohorts combined (2.8%).

Functional Analysis of *greb1l* Variants in Zebrafish

GREB1L encodes growth regulation by estrogen in breast cancer 1 like, a protein of poorly understood function. Consultation of transcriptomic data from the Genitourinary Development Molecular Anatomy Project (GUDMAP) demonstrated that *Greb1l* is expressed robustly in murine metanephric mesenchyme at embryonic day 11.5. It is also expressed in the genital tubercule but not in other lower urinary tract structures. We confirmed expression of *Greb1l* in developing murine kidney, ureter, and bladder (embryonic day 15, Figure S2). The human protein atlas reports nonspecific expression with two commercial antibodies. We also attempted to examine expression by immunohistochemistry but failed to detect a specific signal in human and mouse tissue with a custom antibody. Analysis of transcriptome human adult tissue from Genotype-Tissue Expression (GTEx) demonstrates highest expression in testes and thyroid gland and minimal expression in liver and kidney. There are no other data in mammalian expression or function, but prior studies implicated *greb1l* expression in Hoxb1 and Shha signaling in zebrafish.[57,58]

To test directly whether *GREB1L* has a role in renal morphogenesis and to assess the impact of discovered alleles, we generated a zebrafish model. Reciprocal BLAST analysis with human *GREB1L* identified a single zebrafish *greb1l* ortholog (61% amino acid identity; 73% similarity), against which we designed a splice blocking MO targeting the splice donor site of exon 17 (Figures S3A–S3C). RT-PCR and subsequent sequencing of cDNA from injected embryos showed the MO to be efficient, almost completely abolishing endogenous *greb1l* mRNA and inducing the generation of a message missing exon 17 and terminating translation in exon 18 (of 34). Next, we injected WT embryos (n = 50/injection, replicated) with progressively increasing MO doses (1, 2, 3, and 4 ng) and at 4 dpf we fixed and incubated larvae with an antibody against Na^+-K^+-ATPase that stains the pronephros.[14,45] We then imaged renal structures and we

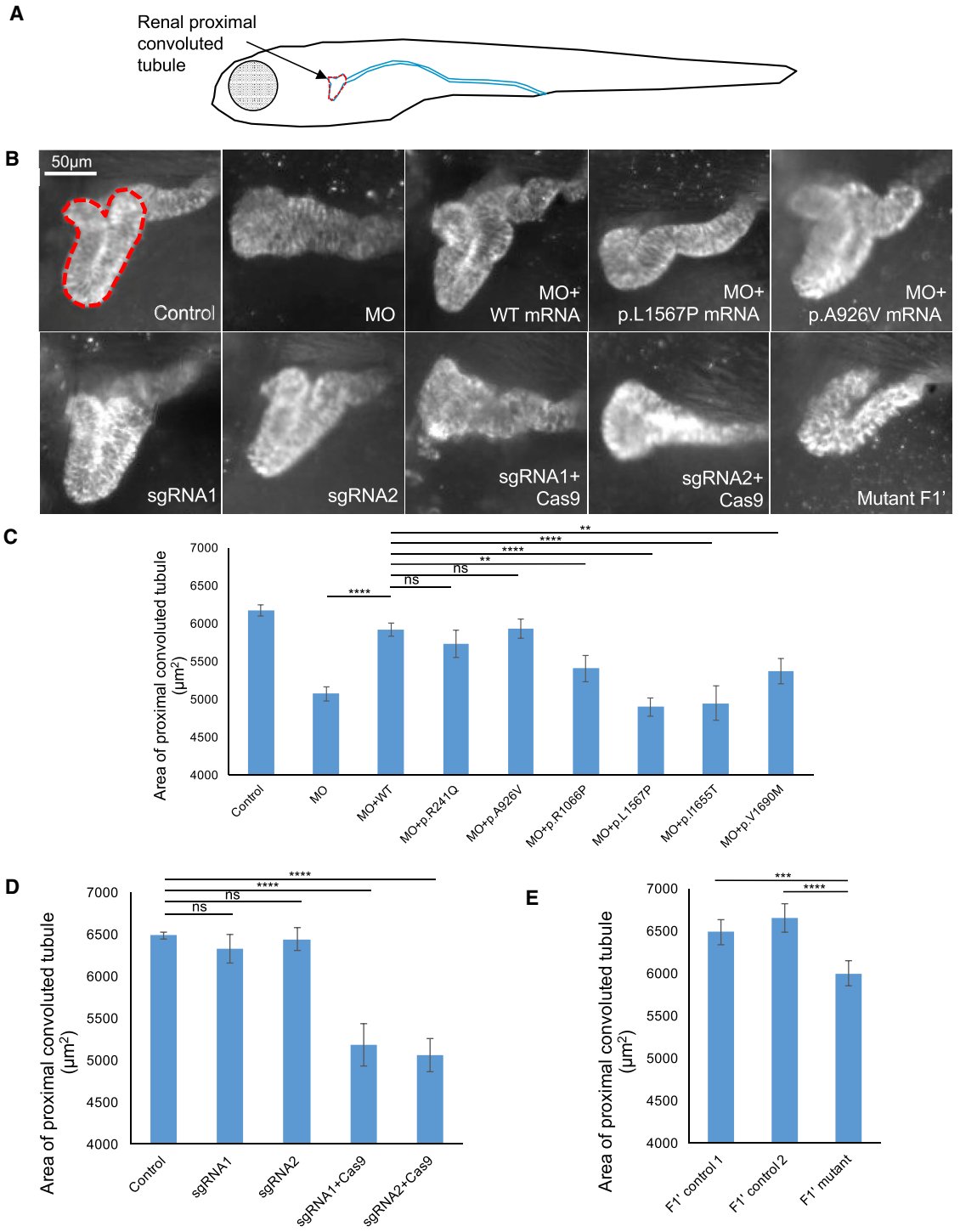

Figure 3. Suppression or Mutation of *greb1l* in Zebrafish Results in Renal Hypoplasia

(A) Schematic of a 4-day post fertilization zebrafish larva (dpf; lateral view); renal tubule is outlined in blue with the proximal convolution shown in red (arrow).

(B) Representative fluorescent images of renal proximal convoluted tubules immunostained with Na^+-K^+-ATPase antibody (a6F) in 4 dpf larvae. Red dashed line in the upper left panel indicates the region measured.

(C–E) Quantification of proximal renal tubule size as indicated by measurement of lateral images (see B). Statistical differences were calculated with a Student's t test and are indicated with ns (not significant), **$p < 0.01$, ***$p < 0.001$, ****$p < 0.0001$.

Abbreviations are as follows: MO, morpholino; WT, wild-type; sgRNA, single guide RNA; F1', progeny of two sgRNA1 F0 mutants. p.R241Q (p.Arg241Gln; rs147048716) and p.A926V (p.Ala926Val; rs569900756) present in controls are benign (minor allele frequency 0.0001053 and 0.001361 in gnomAD, respectively). p.R1066P (p.Arg1066Pro; hypomorph), p.L1567P (p.Leu1567Pro; null), p.I1655T (p.Ile1655Thr; null), and p.V1690M (p.Val1690Met; hypomorph) are exclusive to RHD-affected case subjects. Error bars represent standard error of the mean (SEM); n = 31–55 larvae/batch, repeated; see Table S7 for details.

quantified the area of the proximal renal convoluted tubule. We observed progressive, dose-dependent reduction of this structure (Figures 3B and S3D, Table S7). As a direct test of specificity, we rescued this pathology by co-injecting 2 ng of MO with 200 pg of human *GREB1L* WT mRNA (which by itself did not result in a phenotype; Figures 3C and S3, Table S7).

To validate our transient reagent, we generated *greb1l* CRISPR mutants. Injection of either of two non-overlapping guide (g)RNAs (against exons 8 and 10, respectively) and Cas9 protein into the cell of 1-cell stage embryos yielded F0 mutants with high mosaicism (95%–100% of mRNAs sequenced from four embryos per sgRNA carried insertion/deletion [indel] mutations proximal to the PAM; Figures S3E–S3H). Phenotypic analysis of F0 mutants recapitulated the morphant phenotype, both qualitatively and quantitatively (Figures 3B and 3D, Table S7). Moreover, upon intercrossing F0 adults into the F1′ generation, we observed persistence of the renal phenotype in larval batches of animals bearing a *greb1l* 4 bp deletion (c.827_830delGCAT) in exon 8 (Figure 3B, Table S7).

We next used *in vivo* complementation in morphants to test the pathogenicity of variants discovered in RHD-affected case subjects. We chose four amino acid substitutions detected in case subjects (p.Arg1066Pro, p.Leu1567Pro, p.Ile1655Thr, and p.Val1690Met) and two control variants present at low frequency in ExAC (p.Arg241Gln, p.Ala926Val). In each instance, we asked whether co-injection of MO with human mRNA bearing each of the six variants could rescue the renal pathology similar to controls. Replicate testing showed that the mRNA harboring the control alleles complemented the morphant phenotype whereas the four variants originating from affected individuals failed to rescue the convolution defects (Figure 3C, Table S7). Together, these data support a role for *GREB1L* in renal morphogenesis and provide biological evidence for the pathogenic potential of some of the discovered missense variants.

Discussion

We conducted whole-exome or targeted sequencing in a total of 612 RHD-affected case subjects and compared results to more than 140,000 publicly available as well as to 6,905 internal control subjects to define the mutational landscape of RHD. Using highly rigorous ACMG criteria, annotation of variants in genes known to cause human CAKUT or diseases that might phenocopy kidney malformations resulted in the identification of pathogenic mutations in 7/202 case subjects (3.5%). These mutations affected six known genes. Of these, five are known susceptibility genes for CAKUT, while mutations in *UMOD* gives rise to medullary cystic disease (MIM: 603860),[59] a condition characterized by tubulointerstitial disease and renal failure that can result in atrophic kidneys and may be misdiagnosed as RHD. These data are consistent with prior studies showing mutations in known genes in very variable proportion of CAKUT-affected case subjects, ranging from 1% to 17%.[18,21,60]

Next, we identified unique rare LOF variants in five genes that are either implicated in human multiorgan syndromes (*SETBP1*, *WNT5A*) or whose inactivation in the mouse results in kidney and urinary tract malformations (*SLIT3*, *HSPA4L*, *T*). Most convincingly, the homozygous *SLIT3* c.1193delC mutation (p.Thr398Serfs*37) was found in an affected individual with right renal agenesis, left vesicoureteral reflux, kidney cysts, and patent foramen ovale. The variant was inherited from two heterozygous parents, is absent in all population and internal control subjects, and was predicted to result in premature termination of the protein. Members of the *Slit* gene family encode guidance molecules that interact with roundabout (Robo) homolog receptors to regulate cell migration during neural, cardiac, and renal development.[61–63] Mice harboring *Slit3* homozygous mutations display phenotypes reminiscent of those reported in the affected individual from our cohort, as well as congenital diaphragmatic hernia.[51] Our data implicate mutations in *SLIT3* as a recessive form of human CAKUT, and the identification of additional RHD-affected case subjects with biallelic *SLIT3* mutations will further confirm these findings.

Exome-wide association studies offer a powerful approach to identify disease-causing genes. This design was made possible by the availability of a large in-house control exome dataset and a rigorous analytic pipeline that harmonized sequence coverage between case and control subjects. The availability of external population databases also enabled rapid elimination of common variants from the cohorts, restricting the analysis to novel variants with a higher likelihood of deleteriousness. The top signal was in *GREB1L*, which harbored three LOF variants in case subjects and none in control subjects ($p = 2.0 \times 10^{-5}$). When we introduced novel missense deleterious substitutions as qualifying variants (absent from public databases such as EVS, ExAC, gnomAD, and 1000 Genomes), the strength for association increased to near-exome-wide significance ($p = 4.1 \times 10^{-6}$; OR 8.7). *Post hoc* incorporation of segregation and *de novo* probabilities with the results from our collapsing analysis yielded highly statistical significant evidence for genetic association ($p = 2.3 \times 10^{-7}$), strongly implicating dominant mutations in *GREB1L* as a cause of RHD. Targeted resequencing of *GREB1L* in additional 410 case subjects with renal agenesis or hypodysplasia identified eight additional novel deleterious variants, including a fourth truncating mutation (c.3295C>T [p.Gln1099*]), which again was inherited from an affected parent. Altogether *GREB1L* mutations were identified in 2.8% of RHD-affected case subjects in our cohort, and the finding of four LOF mutations suggests haploinsufficiency as the mechanism leading to the phenotype.

The precise function of GREB1L is not known. It has sequence homology to *GREB1*, an estrogen-regulated

gene expressed in hormone-responsive breast cancer[64] that is expressed in the distal renal vesicle during nephrogenesis.[65] Prior studies have identified that *greb1l* is positively regulated by a Hoxb1 and Shha signaling in zebrafish, implicating *greb1l* in two pathways known to be important for nephrogenesis.[57,58] To determine pathophysiological relevance of *GREB1L* to RHD and to interpret the effect of novel missense mutations, we conducted transient suppression and CRISPR/Cas9 genome editing studies of *greb1l* in zebrafish embryos. We used a direct anatomical surrogate, the convolution of the proximal pronephric tubule, as an established readout for CAKUT.[14,45] CRISPR/Cas9 deletions of *greb1l* in F0 mutants and MO-induced suppression resulted in pronephric convolution defects that were reproducible and specific (the latter rescued by re-introduction of human *GREB1L* mRNA), thus establishing *GREB1L* as a susceptibility gene for RHD. We did not observe *in vivo* complementation with mRNA containing alleles derived from RHD-affected case subjects; however, randomly selected rare missense variants from ExAC complemented the phenotype. Our *GREB1L* findings pose additional questions about its cellular and molecular function and further studies will be required to define its cellular localization, interacting partners, and involvement in developmental processes of the kidney.

In summary, we describe a multi-tiered study (whole-exome case-control study followed by targeted sequencing) involving 612 RHD-affected case subjects and 6,905 control subjects. Our data provide insight into the genetically heterogeneous mutational landscape of human CAKUT and provide evidence for the identification of *SLIT3* and *GREB1L* as disease susceptibility genes. Recently, dominant mutations in GREB1L were identified in independent families segregating dominant kidney malformations.[68] Because RHD can have incomplete penetrance, we suspect that functionalization of additional *GREB1L* variants found in case subjects but present at low frequency in control subjects will identify additional pathogenic mutations and will potentially increase the contribution of this locus to RHD. Future studies of the genetic architecture of RHD will require larger cohorts for discovery of new genes and consideration of noncoding sequence variants, or additional inheritance patterns, such as somatic mosaicism and oligogenic inheritance.

Supplemental Data

Supplemental Data include four figures, seven tables, and Supplemental Acknowledgments and can be found with this article online at https://doi.org/10.1016/j.ajhg.2017.09.018.

Acknowledgments

We thank all individuals with RHD and their family members for participating to this study. This work was supported by grants from the National Institutes of Health (R01DK103184 and UL1 TR000040 to S.S.-C.; R01DK108805 to M.G.S.; R01DK088767 to F.H.; P50DK096415 to N.K.; P30DK096493 to N.K. and E.E.D.; R01DK080099 to A.G.G.; U54DK104309 to A.G.G.; R01DK105124 to K. Kiryluk), the American Heart Association grant-in-aid 13GRNT14680075 to S.S.-C., the Joint Italian Ministry of Health and NIH Young Investigators Finalized Research 2012 to S.S.-C. and G.M.G., the National Human Genome Research Institute Centers for Mendelian Genomics (HG006504 to R.P.L.), and the Fondazione Malattie Renali nel Bambino (to G.M.G.). M.G.S. is supported by the Charles Woodson Clinical Research Fund. A.-M.K. and A.L.-B. are funded by the Polish Ministry of Health. We acknowledge the Polish Kidney Genetics Network (POLYGENES), the Polish Registry of Congenital Malformations (PRCM), the NZOZ Center for Medical Genetics (GENESIS) in Poznań, Poland, and the Dutch Kidney Foundation for the Kolff post-doc abroad grant (15OKK95 to R.W.). The list of contributors for the 6,905 exome controls used in this study is available in the Supplemental Data.

Received: July 25, 2017
Accepted: September 22, 2017
Published: November 2, 2017

Web Resources

1000 Genomes, http://www.internationalgenome.org/
Annotated Variants (ATAV) analyses, https://redmine.igm.cumc.columbia.edu/projects/atav/wiki
CADD, http://cadd.gs.washington.edu/
Centers for Mendelian Genomics, http://www.mendelian.org/
CHOPCHOP, http://chopchop.cbu.uib.no/
ClinVar, https://www.ncbi.nlm.nih.gov/clinvar/
dbSNP, https://www.ncbi.nlm.nih.gov/projects/SNP/
Ensembl Genome Browser, http://www.ensembl.org/index.html
ExAC Browser, http://exac.broadinstitute.org/
GenBank, https://www.ncbi.nlm.nih.gov/genbank/
GenitoUrinary Molecular Anatomy Project (GUDMAP), http://www.gudmap.org/
gnomAD Browser, http://gnomad.broadinstitute.org/
GTEx Portal, https://www.gtexportal.org/home/
Human Gene Mutation Database, http://www.hgmd.cf.ac.uk/ac/index.php
NHLBI Exome Sequencing Project (ESP) Exome Variant Server, http://evs.gs.washington.edu/EVS/
OMIM, http://www.omim.org/
PolyPhen-2, http://genetics.bwh.harvard.edu/pph2/

References

1. Ardissino, G., Daccò, V., Testa, S., Bonaudo, R., Claris-Appiani, A., Taioli, E., Marra, G., Edefonti, A., Sereni, F.; and ItalKid Project (2003). Epidemiology of chronic renal failure in children: data from the ItalKid project. Pediatrics *111*, e382–e387.
2. Collins, A.J., Foley, R.N., Herzog, C., Chavers, B., Gilbertson, D., Herzog, C., Ishani, A., Johansen, K., Kasiske, B., Kutner, N., et al. (2013). US Renal Data System 2012 Annual Data Report. Am. J. Kidney Dis. *61* (1, Suppl 1), A7, e1–e476.
3. Miklovicova, D., Cornelissen, M., Cransberg, K., Groothoff, J.W., Dedik, L., and Schroder, C.H. (2005). Etiology and epidemiology of end-stage renal disease in Dutch children 1987-2001. Pediatr. Nephrol. *20*, 1136–1142.
4. Sanna-Cherchi, S., Ravani, P., Corbani, V., Parodi, S., Haupt, R., Piaggio, G., Innocenti, M.L., Somenzi, D., Trivelli, A., Caridi,

G., et al. (2009). Renal outcome in patients with congenital anomalies of the kidney and urinary tract. Kidney Int. *76*, 528–533.
5. Westland, R., Schreuder, M.F., Bökenkamp, A., Spreeuwenberg, M.D., and van Wijk, J.A. (2011). Renal injury in children with a solitary functioning kidney–the KIMONO study. Nephrol. Dial. Transplant. *26*, 1533–1541.
6. Westland, R., Schreuder, M.F., van Goudoever, J.B., Sanna-Cherchi, S., and van Wijk, J.A. (2014). Clinical implications of the solitary functioning kidney. Clin. J. Am. Soc. Nephrol. *9*, 978–986.
7. Wühl, E., van Stralen, K.J., Verrina, E., Bjerre, A., Wanner, C., Heaf, J.G., Zurriaga, O., Hoitsma, A., Niaudet, P., Palsson, R., et al. (2013). Timing and outcome of renal replacement therapy in patients with congenital malformations of the kidney and urinary tract. Clin. J. Am. Soc. Nephrol. *8*, 67–74.
8. Livera, L.N., Brookfield, D.S., Egginton, J.A., and Hawnaur, J.M. (1989). Antenatal ultrasonography to detect fetal renal abnormalities: a prospective screening programme. BMJ *298*, 1421–1423.
9. Barakat, A.J., and Drougas, J.G. (1991). Occurrence of congenital abnormalities of kidney and urinary tract in 13,775 autopsies. Urology *38*, 347–350.
10. Goodyer, P.R. (2004). Renal dysplasia/hypoplasia. In Pediatric Nephrology, 5th ed., E.D. Avner, W.E. Harmon, and P. Niaudet, eds. (Philadelphia: Lippincott Williams & Wilkins), pp. 83–91.
11. Sanna-Cherchi, S., Sampogna, R.V., Papeta, N., Burgess, K.E., Nees, S.N., Perry, B.J., Choi, M., Bodria, M., Liu, Y., Weng, P.L., et al. (2013). Mutations in DSTYK and dominant urinary tract malformations. N. Engl. J. Med. *369*, 621–629.
12. Thomas, R., Sanna-Cherchi, S., Warady, B.A., Furth, S.L., Kaskel, F.J., and Gharavi, A.G. (2011). HNF1B and PAX2 mutations are a common cause of renal hypodysplasia in the CKiD cohort. Pediatr. Nephrol. *26*, 897–903.
13. Vivante, A., Kleppa, M.J., Schulz, J., Kohl, S., Sharma, A., Chen, J., Shril, S., Hwang, D.Y., Weiss, A.C., Kaminski, M.M., et al. (2015). Mutations in TBX18 cause dominant urinary tract malformations via transcriptional dysregulation of ureter development. Am. J. Hum. Genet. *97*, 291–301.
14. Lopez-Rivera, E., Liu, Y.P., Verbitsky, M., Anderson, B.R., Capone, V.P., Otto, E.A., Yan, Z., Mitrotti, A., Martino, J., Steers, N.J., et al. (2017). Genetic drivers of kidney defects in the DiGeorge syndrome. N. Engl. J. Med. *376*, 742–754.
15. Sanna-Cherchi, S., Kiryluk, K., Burgess, K.E., Bodria, M., Sampson, M.G., Hadley, D., Nees, S.N., Verbitsky, M., Perry, B.J., Sterken, R., et al. (2012). Copy-number disorders are a common cause of congenital kidney malformations. Am. J. Hum. Genet. *91*, 987–997.
16. Verbitsky, M., Sanna-Cherchi, S., Fasel, D.A., Levy, B., Kiryluk, K., Wuttke, M., Abraham, A.G., Kaskel, F., Köttgen, A., Warady, B.A., et al. (2015). Genomic imbalances in pediatric patients with chronic kidney disease. J. Clin. Invest. *125*, 2171–2178.
17. Westland, R., Verbitsky, M., Vukojevic, K., Perry, B.J., Fasel, D.A., Zwijnenburg, P.J., Bökenkamp, A., Gille, J.J., Saraga-Babic, M., Ghiggeri, G.M., et al. (2015). Copy number variation analysis identifies novel CAKUT candidate genes in children with a solitary functioning kidney. Kidney Int. *88*, 1402–1410.
18. Hwang, D.Y., Dworschak, G.C., Kohl, S., Saisawat, P., Vivante, A., Hilger, A.C., Reutter, H.M., Soliman, N.A., Bogdanovic, R., Kehinde, E.O., et al. (2014). Mutations in 12 known dominant disease-causing genes clarify many congenital anomalies of the kidney and urinary tract. Kidney Int. *85*, 1429–1433.
19. Saisawat, P., Kohl, S., Hilger, A.C., Hwang, D.Y., Yung Gee, H., Dworschak, G.C., Tasic, V., Pennimpede, T., Natarajan, S., Sperry, E., et al. (2014). Whole-exome resequencing reveals recessive mutations in TRAP1 in individuals with CAKUT and VACTERL association. Kidney Int. *85*, 1310–1317.
20. Sanna-Cherchi, S., Caridi, G., Weng, P.L., Dagnino, M., Seri, M., Konka, A., Somenzi, D., Carrea, A., Izzi, C., Casu, D., et al. (2007). Localization of a gene for nonsyndromic renal hypodysplasia to chromosome 1p32-33. Am. J. Hum. Genet. *80*, 539–549.
21. Nicolaou, N., Pulit, S.L., Nijman, I.J., Monroe, G.R., Feitz, W.F., Schreuder, M.F., van Eerde, A.M., de Jong, T.P., Giltay, J.C., van der Zwaag, B., et al. (2016). Prioritization and burden analysis of rare variants in 208 candidate genes suggest they do not play a major role in CAKUT. Kidney Int. *89*, 476–486.
22. Cirulli, E.T., Lasseigne, B.N., Petrovski, S., Sapp, P.C., Dion, P.A., Leblond, C.S., Couthouis, J., Lu, Y.F., Wang, Q., Krueger, B.J., et al.; FALS Sequencing Consortium (2015). Exome sequencing in amyotrophic lateral sclerosis identifies risk genes and pathways. Science *347*, 1436–1441.
23. Petrovski, S., Todd, J.L., Durheim, M.T., Wang, Q., Chien, J.W., Kelly, F.L., Frankel, C., Mebane, C.M., Ren, Z., Bridgers, J., et al. (2017). An exome sequencing study to assess the role of rare genetic variation in pulmonary fibrosis. Am. J. Respir. Crit. Care Med. *196*, 82–93.
24. Epi4K consortium; and Epilepsy Phenome/Genome Project (2017). Ultra-rare genetic variation in common epilepsies: a case-control sequencing study. Lancet Neurol. *16*, 135–143.
25. Stitziel, N.O., Stirrups, K.E., Masca, N.G., Erdmann, J., Ferrario, P.G., König, I.R., Weeke, P.E., Webb, T.R., Auer, P.L., Schick, U.M., et al.; Myocardial Infarction Genetics and CARDIoGRAM Exome Consortia Investigators (2016). Coding variation in ANGPTL4, LPL, and SVEP1 and the risk of coronary disease. N. Engl. J. Med. *374*, 1134–1144.
26. Do, R., Stitziel, N.O., Won, H.H., Jørgensen, A.B., Duga, S., Angelica Merlini, P., Kiezun, A., Farrall, M., Goel, A., Zuk, O., et al.; NHLBI Exome Sequencing Project (2015). Exome sequencing identifies rare LDLR and APOA5 alleles conferring risk for myocardial infarction. Nature *518*, 102–106.
27. Lee, S., Abecasis, G.R., Boehnke, M., and Lin, X. (2014). Rare-variant association analysis: study designs and statistical tests. Am. J. Hum. Genet. *95*, 5–23.
28. Ionita-Laza, I., Capanu, M., De Rubeis, S., McCallum, K., and Buxbaum, J.D. (2014). Identification of rare causal variants in sequence-based studies: methods and applications to VPS13B, a gene involved in Cohen syndrome and autism. PLoS Genet. *10*, e1004729.
29. Guo, M.H., Dauber, A., Lippincott, M.F., Chan, Y.M., Salem, R.M., and Hirschhorn, J.N. (2016). Determinants of power in gene-based burden testing for monogenic disorders. Am. J. Hum. Genet. *99*, 527–539.
30. Lek, M., Karczewski, K.J., Minikel, E.V., Samocha, K.E., Banks, E., Fennell, T., O'Donnell-Luria, A.H., Ware, J.S., Hill, A.J., Cummings, B.B., et al.; Exome Aggregation Consortium (2016). Analysis of protein-coding genetic variation in 60,706 humans. Nature *536*, 285–291.
31. Westland, R., Bodria, M., Carrea, A., Lata, S., Scolari, F., Fremeaux-Bacchi, V., D'Agati, V.D., Lifton, R.P., Gharavi, A.G.,

Ghiggeri, G.M., and Sanna-Cherchi, S. (2014). Phenotypic expansion of DGKE-associated diseases. J. Am. Soc. Nephrol. *25*, 1408–1414.
32. Choi, M., Scholl, U.I., Ji, W., Liu, T., Tikhonova, I.R., Zumbo, P., Nayir, A., Bakkaloğlu, A., Ozen, S., Sanjad, S., et al. (2009). Genetic diagnosis by whole exome capture and massively parallel DNA sequencing. Proc. Natl. Acad. Sci. USA *106*, 19096–19101.
33. Halbritter, J., Diaz, K., Chaki, M., Porath, J.D., Tarrier, B., Fu, C., Innis, J.L., Allen, S.J., Lyons, R.H., Stefanidis, C.J., et al. (2012). High-throughput mutation analysis in patients with a nephronophthisis-associated ciliopathy applying multiplexed barcoded array-based PCR amplification and next-generation sequencing. J. Med. Genet. *49*, 756–767.
34. Halbritter, J., Porath, J.D., Diaz, K.A., Braun, D.A., Kohl, S., Chaki, M., Allen, S.J., Soliman, N.A., Hildebrandt, F., Otto, E.A.; and GPN Study Group (2013). Identification of 99 novel mutations in a worldwide cohort of 1,056 patients with a nephronophthisis-related ciliopathy. Hum. Genet. *132*, 865–884.
35. Gillies, C.E., Otto, E.A., Vega-Warner, V., Robertson, C.C., Sanna-Cherchi, S., Gharavi, A., Crawford, B., Bhimma, R., Winkler, C., Kang, H.M., Sampson, M.G.; Nephrotic Syndrome Study Network (NEPTUNE); and C-PROBE InvestigatorGroup of the Michigan Kidney Translational Core Center (2016). tarSVM: Improving the accuracy of variant calls derived from microfluidic PCR-based targeted next generation sequencing using a support vector machine. BMC Bioinformatics *17*, 233.
36. Wang, K., Li, M., and Hakonarson, H. (2010). ANNOVAR: functional annotation of genetic variants from high-throughput sequencing data. Nucleic Acids Res. *38*, e164.
37. Cingolani, P., Platts, A., Wang, L., Coon, M., Nguyen, T., Wang, L., Land, S.J., Lu, X., and Ruden, D.M. (2012). A program for annotating and predicting the effects of single nucleotide polymorphisms, SnpEff: SNPs in the genome of Drosophila melanogaster strain w1118; iso-2; iso-3. Fly (Austin) *6*, 80–92.
38. Adzhubei, I.A., Schmidt, S., Peshkin, L., Ramensky, V.E., Gerasimova, A., Bork, P., Kondrashov, A.S., and Sunyaev, S.R. (2010). A method and server for predicting damaging missense mutations. Nat. Methods *7*, 248–249.
39. Kircher, M., Witten, D.M., Jain, P., O'Roak, B.J., Cooper, G.M., and Shendure, J. (2014). A general framework for estimating the relative pathogenicity of human genetic variants. Nat. Genet. *46*, 310–315.
40. Richards, S., Aziz, N., Bale, S., Bick, D., Das, S., Gastier-Foster, J., Grody, W.W., Hegde, M., Lyon, E., Spector, E., et al.; ACMG Laboratory Quality Assurance Committee (2015). Standards and guidelines for the interpretation of sequence variants: a joint consensus recommendation of the American College of Medical Genetics and Genomics and the Association for Molecular Pathology. Genet. Med. *17*, 405–424.
41. Price, A.L., Patterson, N.J., Plenge, R.M., Weinblatt, M.E., Shadick, N.A., and Reich, D. (2006). Principal components analysis corrects for stratification in genome-wide association studies. Nat. Genet. *38*, 904–909.
42. Samocha, K.E., Robinson, E.B., Sanders, S.J., Stevens, C., Sabo, A., McGrath, L.M., Kosmicki, J.A., Rehnström, K., Mallick, S., Kirby, A., et al. (2014). A framework for the interpretation of de novo mutation in human disease. Nat. Genet. *46*, 944–950.
43. Niederriter, A.R., Davis, E.E., Golzio, C., Oh, E.C., Tsai, I.C., and Katsanis, N. (2013). In vivo modeling of the morbid human genome using *Danio rerio*. J. Vis. Exp., e50338.
44. Shaw, N.D., Brand, H., Kupchinsky, Z.A., Bengani, H., Plummer, L., Jones, T.I., Erdin, S., Williamson, K.A., Rainger, J., Stortchevoi, A., et al. (2017). SMCHD1 mutations associated with a rare muscular dystrophy can also cause isolated arhinia and Bosma arhinia microphthalmia syndrome. Nat. Genet. *49*, 238–248.
45. Bolar, N.A., Golzio, C., Živná, M., Hayot, G., Van Hemelrijk, C., Schepers, D., Vandeweyer, G., Hoischen, A., Huyghe, J.R., Raes, A., et al. (2016). Heterozygous loss-of-function SEC61A1 mutations cause autosomal-dominant tubulointerstitial and glomerulocystic kidney disease with anemia. Am. J. Hum. Genet. *99*, 174–187.
46. Chang, E.H., Menezes, M., Meyer, N.C., Cucci, R.A., Vervoort, V.S., Schwartz, C.E., and Smith, R.J. (2004). Branchio-oto-renal syndrome: the mutation spectrum in EYA1 and its phenotypic consequences. Hum. Mutat. *23*, 582–589.
47. Van Esch, H., Groenen, P., Nesbit, M.A., Schuffenhauer, S., Lichtner, P., Vanderlinden, G., Harding, B., Beetz, R., Bilous, R.W., Holdaway, I., et al. (2000). GATA3 haploinsufficiency causes human HDR syndrome. Nature *406*, 419–422.
48. Sanyanusin, P., Schimmenti, L.A., McNoe, L.A., Ward, T.A., Pierpont, M.E., Sullivan, M.J., Dobyns, W.B., and Eccles, M.R. (1995). Mutation of the PAX2 gene in a family with optic nerve colobomas, renal anomalies and vesicoureteral reflux. Nat. Genet. *9*, 358–364.
49. Ulinski, T., Lescure, S., Beaufils, S., Guigonis, V., Decramer, S., Morin, D., Clauin, S., Deschênes, G., Bouissou, F., Bensman, A., and Bellanné-Chantelot, C. (2006). Renal phenotypes related to hepatocyte nuclear factor-1beta (TCF2) mutations in a pediatric cohort. J. Am. Soc. Nephrol. *17*, 497–503.
50. Hoskins, B.E., Cramer, C.H., Silvius, D., Zou, D., Raymond, R.M., Orten, D.J., Kimberling, W.J., Smith, R.J., Weil, D., Petit, C., et al. (2007). Transcription factor SIX5 is mutated in patients with branchio-oto-renal syndrome. Am. J. Hum. Genet. *80*, 800–804.
51. Liu, J., Zhang, L., Wang, D., Shen, H., Jiang, M., Mei, P., Hayden, P.S., Sedor, J.R., and Hu, H. (2003). Congenital diaphragmatic hernia, kidney agenesis and cardiac defects associated with Slit3-deficiency in mice. Mech. Dev. *120*, 1059–1070.
52. Roifman, M., Marcelis, C.L., Paton, T., Marshall, C., Silver, R., Lohr, J.L., Yntema, H.G., Venselaar, H., Kayserili, H., van Bon, B., et al.; FORGE Canada Consortium (2015). De novo WNT5A-associated autosomal dominant Robinow syndrome suggests specificity of genotype and phenotype. Clin. Genet. *87*, 34–41.
53. Hoischen, A., van Bon, B.W., Gilissen, C., Arts, P., van Lier, B., Steehouwer, M., de Vries, P., de Reuver, R., Wieskamp, N., Mortier, G., et al. (2010). De novo mutations of SETBP1 cause Schinzel-Giedion syndrome. Nat. Genet. *42*, 483–485.
54. Held, T., Paprotta, I., Khulan, J., Hemmerlein, B., Binder, L., Wolf, S., Schubert, S., Meinhardt, A., Engel, W., and Adham, I.M. (2006). Hspa4l-deficient mice display increased incidence of male infertility and hydronephrosis development. Mol. Cell. Biol. *26*, 8099–8108.
55. Pennimpede, T., Proske, J., König, A., Vidigal, J.A., Morkel, M., Bramsen, J.B., Herrmann, B.G., and Wittler, L. (2012). In vivo knockdown of Brachyury results in skeletal defects and

urorectal malformations resembling caudal regression syndrome. Dev. Biol. *372*, 55–67.
56. Sampson, M.G., Gillies, C.E., Ju, W., Kretzler, M., and Kang, H.M. (2013). Gene-level integrated metric of negative selection (GIMS) prioritizes candidate genes for nephrotic syndrome. PLoS ONE *8*, e81062.
57. Xu, J., Srinivas, B.P., Tay, S.Y., Mak, A., Yu, X., Lee, S.G., Yang, H., Govindarajan, K.R., Leong, B., Bourque, G., et al. (2006). Genomewide expression profiling in the zebrafish embryo identifies target genes regulated by Hedgehog signaling during vertebrate development. Genetics *174*, 735–752.
58. Choe, S.K., Zhang, X., Hirsch, N., Straubhaar, J., and Sagerström, C.G. (2011). A screen for hoxb1-regulated genes identifies ppp1r14al as a regulator of the rhombomere 4 Fgf-signaling center. Dev. Biol. *358*, 356–367.
59. Hart, T.C., Gorry, M.C., Hart, P.S., Woodard, A.S., Shihabi, Z., Sandhu, J., Shirts, B., Xu, L., Zhu, H., Barmada, M.M., and Bleyer, A.J. (2002). Mutations of the UMOD gene are responsible for medullary cystic kidney disease 2 and familial juvenile hyperuricaemic nephropathy. J. Med. Genet. *39*, 882–892.
60. Weber, S., Moriniere, V., Knüppel, T., Charbit, M., Dusek, J., Ghiggeri, G.M., Jankauskiené, A., Mir, S., Montini, G., Peco-Antic, A., et al. (2006). Prevalence of mutations in renal developmental genes in children with renal hypodysplasia: results of the ESCAPE study. J. Am. Soc. Nephrol. *17*, 2864–2870.
61. Mommersteeg, M.T., Andrews, W.D., Ypsilanti, A.R., Zelina, P., Yeh, M.L., Norden, J., Kispert, A., Chédotal, A., Christoffels, V.M., and Parnavelas, J.G. (2013). Slit-roundabout signaling regulates the development of the cardiac systemic venous return and pericardium. Circ. Res. *112*, 465–475.
62. Yuan, W., Rao, Y., Babiuk, R.P., Greer, J.J., Wu, J.Y., and Ornitz, D.M. (2003). A genetic model for a central (septum transversum) congenital diaphragmatic hernia in mice lacking Slit3. Proc. Natl. Acad. Sci. USA *100*, 5217–5222.
63. Yuan, W., Zhou, L., Chen, J.H., Wu, J.Y., Rao, Y., and Ornitz, D.M. (1999). The mouse SLIT family: secreted ligands for ROBO expressed in patterns that suggest a role in morphogenesis and axon guidance. Dev. Biol. *212*, 290–306.
64. Ghosh, M.G., Thompson, D.A., and Weigel, R.J. (2000). PDZK1 and GREB1 are estrogen-regulated genes expressed in hormone-responsive breast cancer. Cancer Res. *60*, 6367–6375.
65. Brunskill, E.W., Park, J.S., Chung, E., Chen, F., Magella, B., and Potter, S.S. (2014). Single cell dissection of early kidney development: multilineage priming. Development *141*, 3093–3101.
66. Bellanné-Chantelot, C., Chauveau, D., Gautier, J.F., Dubois-Laforgue, D., Clauin, S., Beaufils, S., Wilhelm, J.M., Boitard, C., Noël, L.H., Velho, G., and Timsit, J. (2004). Clinical spectrum associated with hepatocyte nuclear factor-1beta mutations. Ann. Intern. Med. *140*, 510–517.
67. Bernascone, I., Vavassori, S., Di Pentima, A., Santambrogio, S., Lamorte, G., Amoroso, A., Scolari, F., Ghiggeri, G.M., Casari, G., Polishchuk, R., and Rampoldi, L. (2006). Defective intracellular trafficking of uromodulin mutant isoforms. Traffic *7*, 1567–1579.
68. Brophy, P.D., Rasmussen, M., Parida, M., Bonde, G., Darbro, B.W., Hong, X., Clarke, J.C., Peterson, K.A., Denegre, J., Schneider, M., et al. (2017). A gene implicated in activation of retinoic acid receptor targets is a novel renal agenesis gene in humans. Genetics *207*, 215–228.